Exciton Autoionization in Ion-Induced Electron Emission

N. Bajales, L. Cristina, and S. Mendoza
Instituto de Desarrollo Tecnológico para la Industria Química, CONICET and Universidad Nacional del Litoral. Güemes 3450 CC 91, 3000 Santa Fe, Argentina

R. A. Baragiola
Engineering Physics, University of Virginia, Charlottesville, Virginia 22904, USA

E. C. Goldberg and J. Ferrón
Instituto de Desarrollo Tecnológico para la Industria Química and Departamento de Ingeniería de Materiales, F.I.Q.; CONICET and Universidad Nacional del Litoral. Güemes 3450 CC 91, 3000 Santa Fe, Argentina

(Received 20 February 2008; published 6 June 2008)

We report on measurements of electron emission spectra from surfaces of highly oriented pyrolytic graphite (HOPG) excited by 1–5 keV He^+ and Li^+ which, for He^+, exhibit a previously unreported high-energy structure. Through a full quantum dynamic description that allows for the calculation of neutralization and electron-hole pair excitation, we show that these high-energy electrons can arise from autoionization of excitons formed by electron promotion to conduction band states close to the vacuum level. The same calculation explains the observed absence of high-energy excitons for Li^+ on HOPG.

DOI: 10.1103/PhysRevLett.100.227604 PACS numbers: 79.20.Rf, 68.49.Sf, 71.35.−y, 81.05.Uw

Low-energy ion-surface collisions are of fundamental importance in surface studies. Applications range from sample treatment, as in sputter cleaning or ion depth profiling, to the most surface sensitive techniques, secondary ion mass spectrometry (SIMS) and ion scattering spectroscopy (ISS). Quantification of ISS and SIMS require a deep understanding of electronic processes at the surface, which so far is incomplete. An outcome of electronic processes that can be studied in detail is the emission of electrons from the solid. Since this process is very surface sensitive the electron energy distributions can, in principle, provide rich information on the surface electronic structure. [1]

In the 1–5 keV ion energy range studied here, electron emission occurs either at the expense of the neutralization energy of the ion, known as potential emission, or of its kinetic energy. In the first case, the Coulomb interaction between two electrons in the solid may cause one electron to tunnel the surface barrier to neutralize the incoming ion while the other one is excited. This process, known as Auger neutralization (AN) [1], can result in an electron being emitted outside the solid if the neutralization energy is larger than twice the work function of the surface. In another process, Auger deexcitation (AD), an electron may tunnel to an excited state of the ion and then decay by an Auger process involving one electron from the solid. In addition, there are one-electron resonant neutralization (RN) channels, in which the electron energy remains constant and no electron emission occurs. The probability of AN, AD, and RN decays with ion energy as the time of interaction of the projectile with the surface diminishes. The other process, kinetic electron emission, is similar to ionization in gas-phase collisions, where electrons are promoted into the continuum by the time-varying electric fields during the collision.

To gain insight into the electron emission mechanisms, we can tailor the experiments by a proper selection of the colliding partners, to enhance or suppress particular processes. For instance, He^+ on Al, where the He ionization level lies well below the bottom of the valence band and cannot be filled by RN, has become a model system to study AN. In the case of Al and Mg, the large neutralization energy of He^+ and Ne^+ allows the excitation of plasmons, which are identified through their decay into electrons observed outside the solid [2]. Here we study highly oriented pyrolytic graphite (HOPG), which presents interesting features. In a simple picture where electron transfer occurs between weakly perturbed levels, the uncommonly wide valence band of HOPG allows RN even for He^+, with its large neutralization energy. This mechanism, being much faster than AN, essentially removes AN as a significant source of emitted electrons. In addition, the low density of states of HOPG at the Fermi level prevents, neglecting level perturbation, RN to the first excited state of He. This has led to the conclusion that RN to the ground state is the only possible neutralization channel [3]. Within this model, and considering that HOPG plasmons, even if excited, do not decay through electron emission [4], the only potential mechanism for electron ejection seems to be an intraband, Coster Kronig, Auger process filling the hole in C produced by RN of the He^+ projectile. In this case, the spectrum of electrons emitted by He^+ would be a broad peak extending to ~18 eV (neutralization energy minus twice the surface work function (9.4 eV), plus kinematical broadening [1]). Here, by combined measurements of electron emission and a full quantum dynamic calculation of He$^+$-HOPG and Li$^+$-HOPG interactions, we show that this expectation is quite far from reality. Rather, our work suggests the existence of a new mechanism, the creation of high-energy valence excitons of HOPG by electron promotion in a close He-C collision followed by their autoionization into vacuum.

Our experiments were performed in an electron spectrometer system (PHI SAM 590 A) equipped with a single pass cylindrical energy analyzer, with a base pressure in the low 10^{-10} Torr range. The HOPG sample was introduced in vacuum immediately after cleavage and heated to 1300 K for several minutes. After this treatment no contamination is observed by Auger electron spectroscopy (AES), while low-energy electron diffraction shows sharp circles due to the mosaic structure. Nevertheless, since low-energy electron emission is quite more sensitive to contamination than AES, the ultimate check of the surface state was the repeatability of the electron energy spectra after annealing. The total ion fluence was kept below the threshold for damage that causes changes in either plasmon energy or work function [5]. In addition, at each ion energy we took several spectra at the same and at different surface spots to detect any influence of damage. When damage was detected, the sample was annealed. This procedure was successful except when using Ar projectiles which caused damage that could not be fully healed by annealing and required the use of a new sample.

Figure 1 shows electron energy spectra for HOPG impacted by 1–5 and 2–5 keV He$^+$ and Li$^+$, respectively. The instrument measures $N(E)E$, where $N(E)$ is the number of electrons of energy between E and E^+dE. The spectra shown in Fig. 1 are normalized to the same area and are not corrected for analyzer transmission (proportional to E) to better visualize the energy dependence of the higher energy emission structure. In all cases, the total electron emission yields increase rapidly with ion energy, as expected from kinetic emission mechanisms.

The results of Fig. 1 reveal differences between He$^+$ and Li$^+$ excitations that go beyond those expected from potential emission. While Li$^+$ ions produce electron spectra with the low-energy cascade component typical of kinetic emission, the spectra induced by He$^+$ show, in addition to the AN component extending to ~18 eV, mentioned above, a high-energy structure. The mechanism responsible for these high-energy electrons increases in importance with increasing ion energy above an apparent threshold at ~1.3 keV. This strong projectile-energy dependence allows us to disregard AN, AD, and plasmon deexcitation [4] as the origin of these fast electrons and points to a kinetic emission mechanism. As in other studies [1], we interpret the threshold energy as that at which the distance of closest approach attains a critical value for electron promotion and coupling to unfilled states.

To gain insight about the origin of the high-energy electrons, we performed a quantum dynamical calculation for He$^+$ on HOPG that considers neutralization to both the ground and the first excited states of He, but excludes the negative ion channel that is only observed on alkali-coated (low work function) surfaces [1]. The electron-hole pair excitations in the band and ion neutralization are calculated consistently. Neutralization to He 2s was included because we found that it is needed to reproduce the high neutral fractions measured in ISS experiments [6]. This calculation uses a formalism based on the infinite-correlation approach to the Anderson Hamiltonian [7]. In a simplified picture where the spin of the electron in He$^+$ is frozen, an electron with the same spin can be transferred to form the lowest lying excited state $(1s\uparrow\, 2s\uparrow)^3S$, while another electron with the opposite spin can be transferred to the ground state $(1s\uparrow\, 1s\downarrow)^1S$. We neglect here states lying above He ^3S. The Hamiltonian can be written as

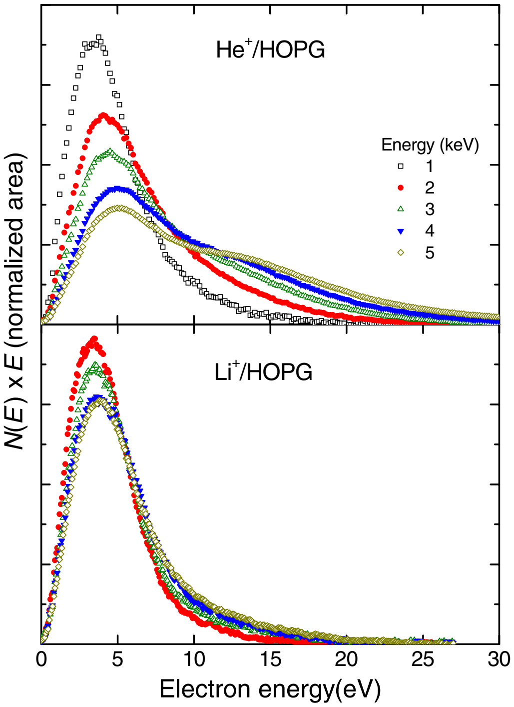

FIG. 1 (color online). Electron energy spectra induced by 1–5 keV He$^+$ and Li$^+$, normalized to the area.

$$H = \sum_{k,\sigma} \varepsilon_k n_{k\sigma} + \sum_{\sigma} E_{a\sigma} n_{a\sigma} + \sum_{k,\sigma} [V_{k,a\sigma} c^\dagger_{k\sigma} b^\dagger c_{a\sigma} + \text{h.c.}]. \tag{1}$$

Where k denotes the solid state levels (valence and core) with energies ε_k, $V_{ka\sigma}$ is the coupling between the solid and atomic state of energy $E_{a\sigma}$, and σ denotes the spin state. The energies corresponding to the 1s and 2s neutral He states are defined as total energy differences:

$$\begin{aligned} E_{a\uparrow} &= E_{tot}(2s\uparrow\, 1s\uparrow) - E_{tot}(1s\uparrow), \\ E_{a\downarrow} &= E_{tot}(1s\downarrow\, 1s\uparrow) - E_{tot}(1s\uparrow). \end{aligned} \tag{2}$$

The boson operators b^+, b ensure the projection on the correct subspace through the constraint relation: $b^+b + \sum_\sigma n_{a\sigma} = 1$.

Then, $\langle n_{a\uparrow}\rangle$ and $\langle n_{a\downarrow}\rangle$ give directly the neutralization probability to the excited and ground states of He, respectively. We calculate the time evolution of the occupation of graphite band states through the expression [7]

$$\frac{d}{dt}\sum_\sigma \langle n_{k\sigma}(t)\rangle = -2\,\mathrm{Im}\sum_\sigma V_{ka\sigma}(t)\langle c^+_{k\sigma} b^+ c_{a\sigma}\rangle_t. \qquad (3)$$

By expanding in (3) the k states in the $2s$ and $2p$ atomic orbital of the C atoms, we obtain $N(\varepsilon, t)$, the electron energy distribution at the surface, from

$$\begin{aligned}\frac{d}{dt}N(\varepsilon, t) &= \sum_\sigma N_\sigma(\varepsilon, t)\\ &= \sum_{\sigma,m,n} -2\,\mathrm{Im}V_{ma\sigma}(t)\rho^\sigma_{mn}(\varepsilon)\langle c^\dagger_{\varepsilon\sigma} b^\dagger c_{a\sigma}\rangle_t, \qquad (4)\end{aligned}$$

where m and n run over the carbon orbitals, $\rho^\sigma_{mn}(\varepsilon)$ is the LSDOS of HOPG [8], and $V_{m,a\sigma}$ is the coupling between He and C states. The initial condition for $N(\varepsilon, t)$, corresponding to the noninteracting He-HOPG surface, is

$$N(\varepsilon, t = -\infty) = \sum_{\sigma,m,n} \rho^\sigma_{\mathrm{mn}}(\varepsilon) f_\prec(\varepsilon),$$

where $f_\prec(\varepsilon)$ is the Fermi distribution. For all times it is verified that

$$\begin{aligned}\int_{-\infty}^{\infty} N(\varepsilon, t)d\varepsilon + \sum_\sigma \langle n_{a\sigma}(t)\rangle &= \int_{-\infty}^{\infty} \sum_{m,n,\sigma} \rho^\sigma_{mn}(\varepsilon) f_\prec(\varepsilon) d\varepsilon\\ &\quad + \sum_\sigma \langle n_{a\sigma}(-\infty)\rangle,\end{aligned}$$

which ensures the conservation of the total number of electrons.

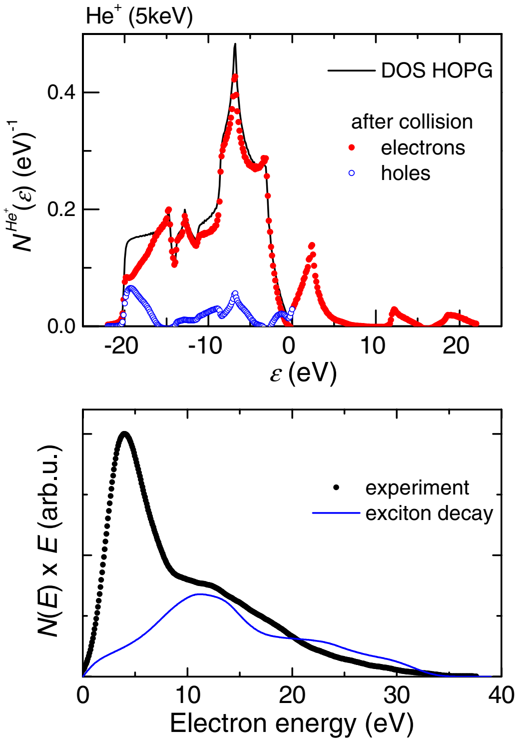

FIG. 2 (color online). Top: Local surface density of states for HOPG, electron energy distribution produced by He$^+$ 5 keV corresponding to He$^+$ final state, and hole distribution below the Fermi level. Bottom—comparison of the contribution to the electron spectra for the autoionization of the HOPG exciton with experimental data. The curves are normalized to facilitate comparison of their shapes.

The electron distribution for the case when He$^+$ is not neutralized may be obtained from the expression $\sum_\sigma\langle c^+_{k\sigma}c_{k\sigma}(1 - c^+_{a\sigma}c_{a\sigma})\rangle$, and calculated approximately using the LCAO-expansion of the surface states, as

$$\begin{aligned}N^{\mathrm{He}^+}(\varepsilon, t) = \sum_\sigma &[N_\sigma(\varepsilon, t)(1 - \langle n_{a\sigma}(t)\rangle)\\ &+ \sum_{m,n}\rho^\sigma_{mn}(\varepsilon)|\langle c^\dagger_{\varepsilon\sigma} b^\dagger c_{a\sigma}\rangle_t|^2].\end{aligned}$$

The energy distribution of directly excited electrons $N(\varepsilon) = N(\varepsilon, t = \infty)$ is calculated for different impact parameters and weighted by the corresponding area (probability of occurrence). A previously developed *bond-pair* model for the interaction is used to calculate the parameters of the Hamiltonian [9].

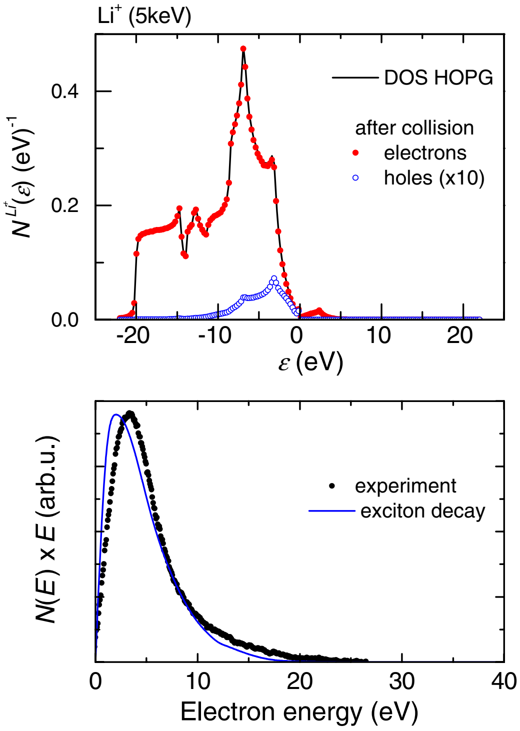

FIG. 3 (color online). The same as Fig. 2 but for 5 keV Li$^+$ on HOPG. Note that the hole distribution is magnified tenfold.

In Fig. 2 we show the LSDOS of HOPG, and the electron distribution $N^{\mathrm{He}^+}(\varepsilon, \infty)$ after the impact of 5 keV He$^+$. One

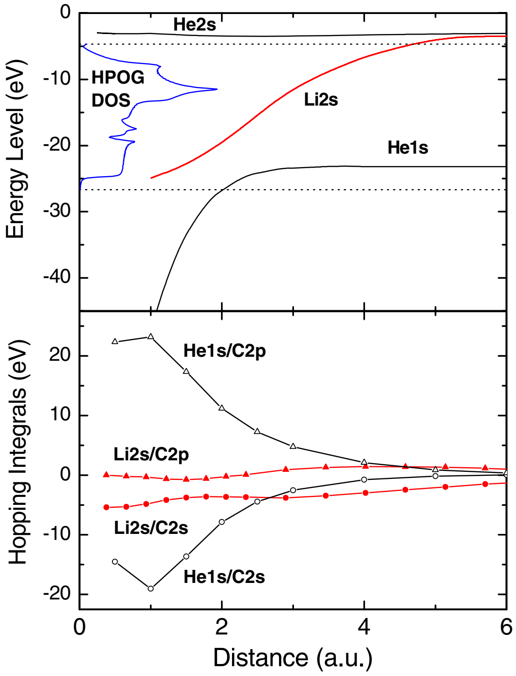

FIG. 4 (color online). Hamiltonian terms for the interaction of Li^+ and He^+ with a HOPG surface as a function of distance to a surface C atom. The horizontal lines mark the extremes of the C-valence band. Top: Energy levels. Bottom: Coupling terms (hopping integrals).

can see the density of hole states generated below the Fermi level and the electron occupation of conduction band states, with a tail extending to energies way above the vacuum level. The shapes of the electron and hole distributions are strongly governed by the peculiar LSDOS of HOPG. We then calculate the autoionization decay spectra, where the energy of recombination of a hole and an electron (exciton) is transferred to another electron in the valence band. The energy distribution of electrons outside the solid is then obtained by considering transmission through the surface barrier [1]. The result of a simple convolution over all band states in the lower part of Fig. 2 shows that the autoionization of excitons can explain the presence of the most energetic electrons of the He^+/HOPG electron emission spectra.

We calculate similarly the electron distribution $N^{\mathrm{Li}^+}(\varepsilon)$ for Li^+-HOPG collisions but considering Li $2s$ as the only projectile state active in the dynamical process and using a spinless approximation of the Anderson Hamiltonian. Figure 3 shows that the excitation of electron-hole pairs comes only from the p-band states close to the Fermi level. If these pairs can be considered as shallow excitons, their autoionization would contribute electrons below ~7 eV, which would be hidden within those from low-energy secondary electron cascade.

To understand the origin of the HOPG valence band electron excitation by He^+, and the different spectra for He^+ and Li^+ projectiles, we show in Fig. 4 the variation of the energy levels and hopping integrals along the ion trajectory. Although we find a pronounced downshift of the energy level for both projectiles, significant promotion of HOPG electrons in Li-C collisions is not expected due to the relatively weak interactions, compared with the He-C case (see the hopping integrals in Fig. 4).

In summary, we found that collisions of He^+ with a HOPG surface results in the emission of energetic electrons extending up to ~30 eV, which increases strongly with projectile energy above a threshold of ~1.3 keV, indicating a kinetic emission mechanism. Using a calculation that takes into account the first excited state of He and correlation effects, we derive the population of excitonic states in HOPG that, through autoionization, provides a possible source for the observed high-energy electrons. Unlike the well-studied core exciton ($1s$) in HOPG [10], the valence exciton proposed here involves a hole in the *valence* band excited through collisions. Its decay through autoionization competes with side filling of the valence hole by electron transfer from neighboring atoms. This side filling, dominant in metals near the Fermi level, is hindered in graphite, as evidenced by the sharpness of structures of the LSDOS [11]. The theory shown here not only explains the presence of high-energy electrons in the secondary spectra, but also the high neutralization probability of He^+ on HOPG observed in ISS experiments [3].

This work was supported by ANPCyT through PICT14730 and 14724, CONICET through PIP 5277, and U.N.L. through CAI+D grants. R. A. B. was supported by the Alice and Guy Wilson endowment.

[1] R. A. Baragiola, in *Low Energy Ion Surface Interaction*, edited by J. W. Rabalais (Wiley, New York, 1994), Chap. 4.
[2] R. A. Baragiola and C. A. Dukes, Phys. Rev. Lett. **76**, 2547 (1996).
[3] L. C. A. van den Oetelaar *et al.*, Nucl. Instrum. Methods Phys. Res., Sect. B **85**, 420 (1994); R. Souda *et al.*, Surf. Sci. **421**, 89 (1999).
[4] A. Hoffman, M. Elbaun, and R. Brener, Phys. Rev. B **48**, 16 078 (1993) ; A. Hoffman and R. Brener, Phys. Rev. B **51**, 1817 (1995)
[5] H. Hashimoto *et al.*, Surf. Interface Anal. **35**, 19 (2003).
[6] N. Bajales, *et al.* J. Mol. Catal. A: Chem. **281**, 237 (2008).
[7] E. C. Goldberg, F. Flores, and R. C. Monreal, Phys. Rev. B **71**, 035112 (2005).
[8] Calculated by C. González Pascual (private communication).from O. F. Sankey and D. J. Niklewski, Phys. Rev. B **40**, 3979 (1989).
[9] P. G. Bolcatto, E. C. Goldberg, and M. C. G. Passeggi, Phys. Rev. A **50**, 4643 (1994).
[10] Y. Ma *et al.*, Phys. Rev. Lett. **71**, 3725 (1993); P. A. Bruhwiler *et al.*, Phys. Rev. Lett. **74**, 614 (1995).
[11] T. Kihlgren *et al.*, Phys. Rev. B **66**, 235422 (2002).